



# IMPACT Parallel Code Suite for Light Source Beam Dynamics Simulation

Ji Qiang

Lawrence Berkeley National Laboratory

Dec. 1, 2006, SLAC

## Theta code:

Linear accelerator lattice design and layout

## Fix3d/2d code:

Envelope matching and analysis

## Impact3d code:

Parallel 3d beam dynamics simulation using position as independent variable

## Impact-T code:

Parallel 3d beam dynamics simulation using time as independent variable

## Preprocessing/Postprocessing codes:

Preparation of Fourier coefficients, slice emittance...

# IMPACT

## (Integrated Map and Particle Accelerator Tracking)



- Started as
  - 3D parallel PIC code
  - Split-operator based with  $H = H_{\text{external}} + H_{\text{space charge}}$
  - 3D space charge w/ 2 types of boundary conditions
  - Linear maps for drifts, quads, rf gaps
  - Maps computed “on the fly” by numerically integrating the equations for the linear transfer map
    - based on well-established methods for computing maps
    - generalization to high order straightforward
    - transformations are symplectic by construction
      - No need for Prome-like corrections for rf gap transformations
  - Reference trajectory equations also computed “on the fly”

# Current Features of IMPACT3d (Z) Code



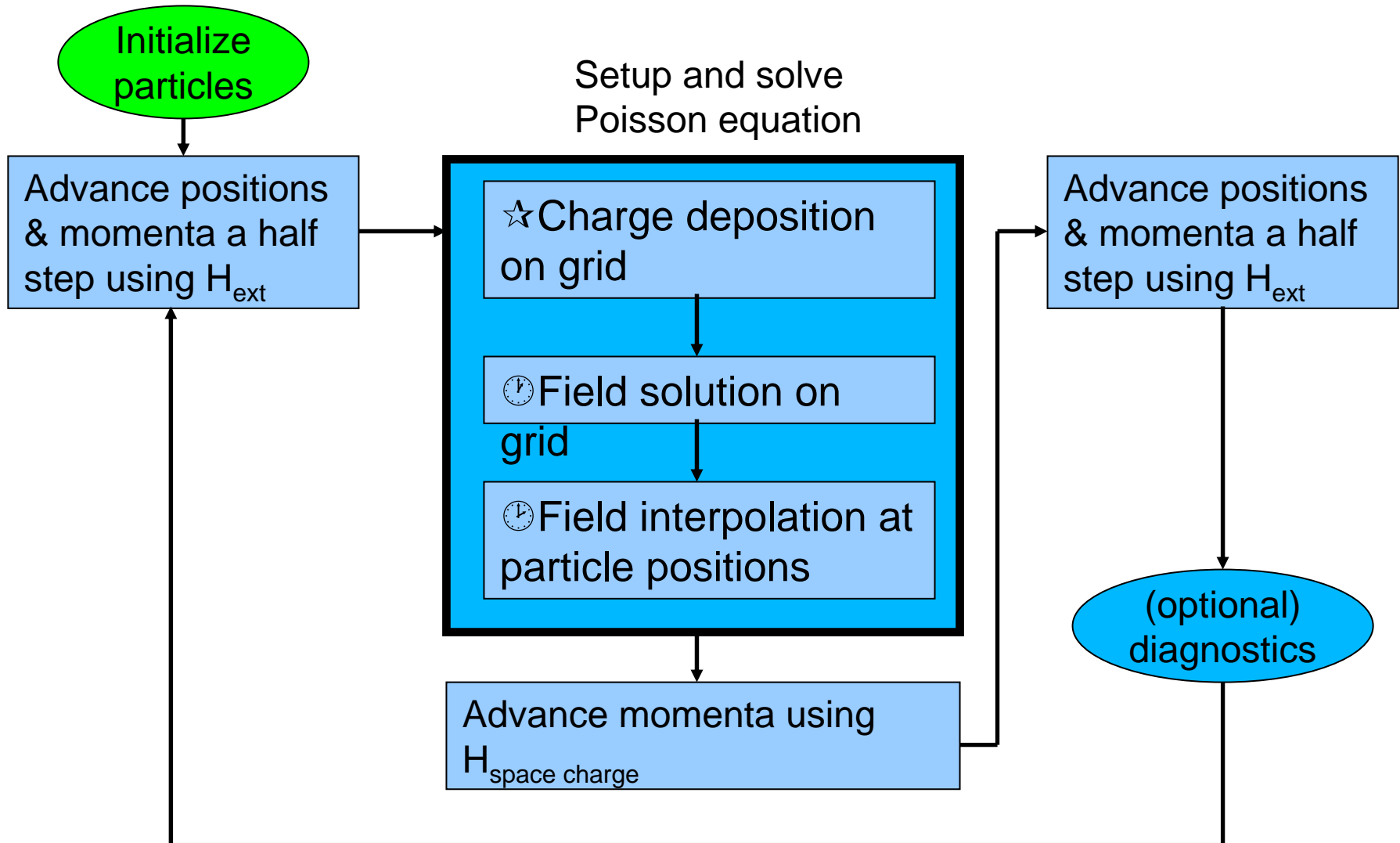
1. Two Numerical Integrators:
  - Linear Map
  - Nonlinear Lorentz Force Integrator (using  $z/t$  as independent variable)
- External Beam Line Elements:
  - Quadrupole, Dipole, Solenoid + RF gap, Sextupole, Octupole, 3D constant focusing channel
  - DTL, CCDTL, CCL, SC, TWS, User-defined element
- 3D Space Charge with 6 Types of Boundary Conditions
- Short range longitudinal and transverse wake
- 1D CSR wake
- Multiple Charge State
- Restart Function and Dynamic Load Balance

# Current Features of IMPACT-T Code



- 3D Integrated Green method to accurately compute the space-charge forces for a beam with large aspect ratio
- 3D Shifted Green method to efficiently compute the space-charge forces from the image charge
- Multiple slices/bins to handle the beam with large energy spread
- Arbitrary overlap of external fields to allow the modeling of both standing wave and traveling wave structure
- Transverse and longitudinal wakefield effects included
- 1D CSR wakefield
- 3D point-to-point N-body model including relativistic effects of individual particle

# Particle-In-Cell (PIC) Simulation



# Green Function Solution of Poisson's Equation

(with 3D Open Boundary Conditions)



$$\phi(r) = \int G(r, r') \rho(r') dr' ; r = (x, y, z)$$

$$\phi(r_i) = h \sum_{i'=1}^N G(r_i - r_{i'}) \rho(r_{i'})$$

$$G(x, y, z) = 1 / \sqrt{(x^2 + y^2 + z^2)}$$

Direct summation of the convolution scales as  $N^6$  !!!!  
N – grid number in each dimension

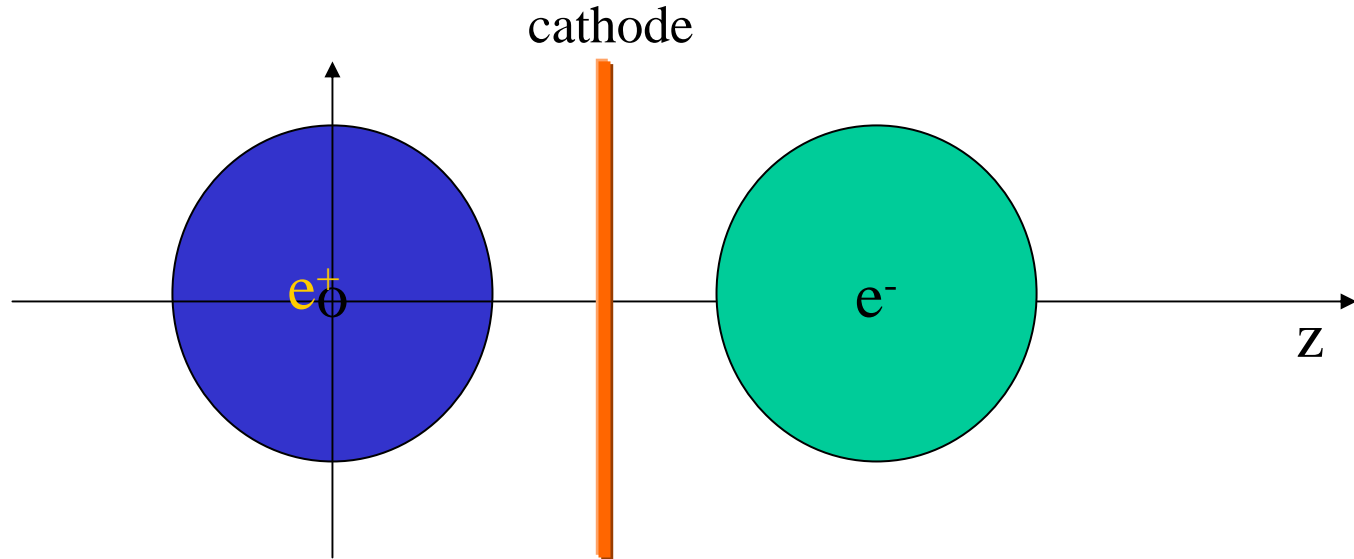
Hockney's Algorithm:- *scales as  $(2N)^3 \log(2N)$*

- Ref: Hockney and Easwood, *Computer Simulation using Particles*, McGraw-Hill Book Company, New York, 1985.

$$\phi_c(r_i) = h \sum_{i'=1}^{2N} G_c(r_i - r_{i'}) \rho_c(r_{i'})$$

$$\phi(r_i) = \phi_c(r_i) \quad \text{for } i = 1, N$$

# A Schematic Plot of an $e^-$ Beam and Its Image Charge



Shifted Green function Algorithm:

$$\phi_F(r) = \int G_s(r, r') \rho(r') dr'$$

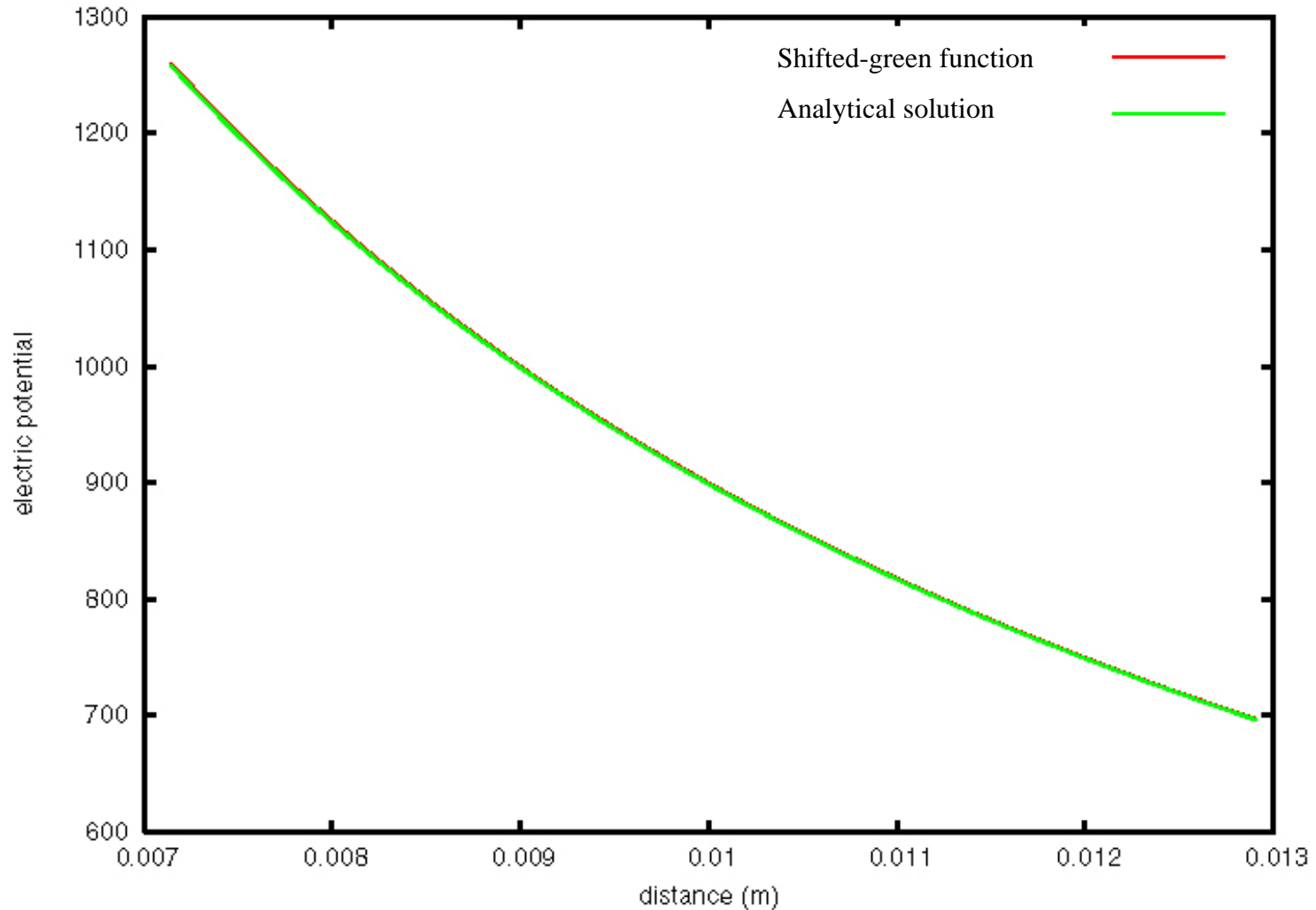
$$G_s(r, r') = G(r + r_s, r')$$

Ref:

1) J. Qiang, M. Furman, and R. Ryne, "Strong-Strong Beam-Beam Simulation Using a Green Function Approach," [Phys. Rev. ST Accel. Beams, vol 5, 104402 \(October 2002\).](#)

2) J. Qiang, S. Lidia, R. D. Ryne, and C. Limborg-Deprey, "A Three-Dimensional Quasi-Static Model for High Brightness Beam Dynamics simulation," [Phys. Rev. ST Accel. Beams, vol 9, 044204 \(2006\).](#)

# Test of Image Space-Charge Calculation Numerical Solution vs. Analytical Solution

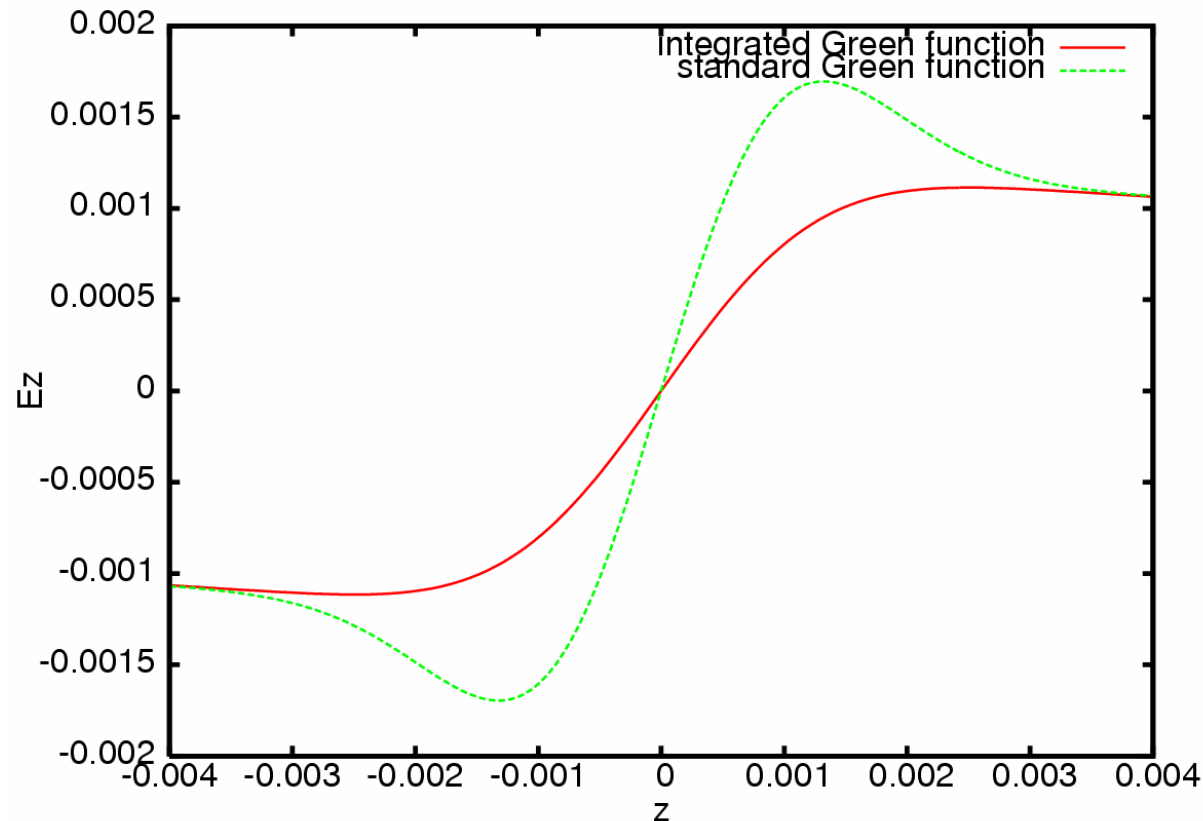


# Integrated Green Function Solution of Poisson's Equation



$$\phi_c(r_i) = \sum_{i'=1}^{2N} G_i(r_i - r_{i'}) \rho_c(r_{i'})$$

$$G_i(r, r') = \oint G_s(r, r') dr'$$



# Spectral Solution of Poisson's Equation

(with Transverse Closed Boundary Conditions)



$$\frac{\partial^2 \phi}{\partial r^2} + \frac{1}{r} \frac{\partial \phi}{\partial r} + \frac{1}{r^2} \frac{\partial^2 \phi}{\partial \theta^2} + \frac{\partial^2 \phi}{\partial z^2} = -\rho$$

$$\phi(r = 1, \theta, z) = 0$$

$$\phi(r, \theta + 2\pi, z) = \phi(r, \theta, z)$$

$$\phi(r, \theta, z = \pm\infty) = 0$$

J. Qiang and R. D. Ryne, "Parallel 3D Poisson Solver for a Charged Beam in a Conducting Pipe," *Comp. Phys. Comm.*, vol 138, p. 138, (2001).

# Spectral Solution of Poisson's Equation



$$\rho(r, \theta, z) = \sum_{m=-N_m/2}^{N_m/2-1} \sum_{l=1}^{N_l} \rho^{lm}(z) J_m(\gamma_{lm} r) \exp(-im\theta)$$

$$\phi(r, \theta, z) = \sum_{m=-N_m/2}^{N_m/2-1} \sum_{l=1}^{N_l} \phi^{lm}(z) J_m(\gamma_{lm} r) \exp(-im\theta)$$

$$\rho^{lm}(z) = \frac{1}{\pi J_m'^2(\gamma_{lm})} \int_0^{2\pi} \int_0^1 \rho(r, \theta, z) \exp(im\theta) r J_m(\gamma_{lm} r) dr d\theta$$

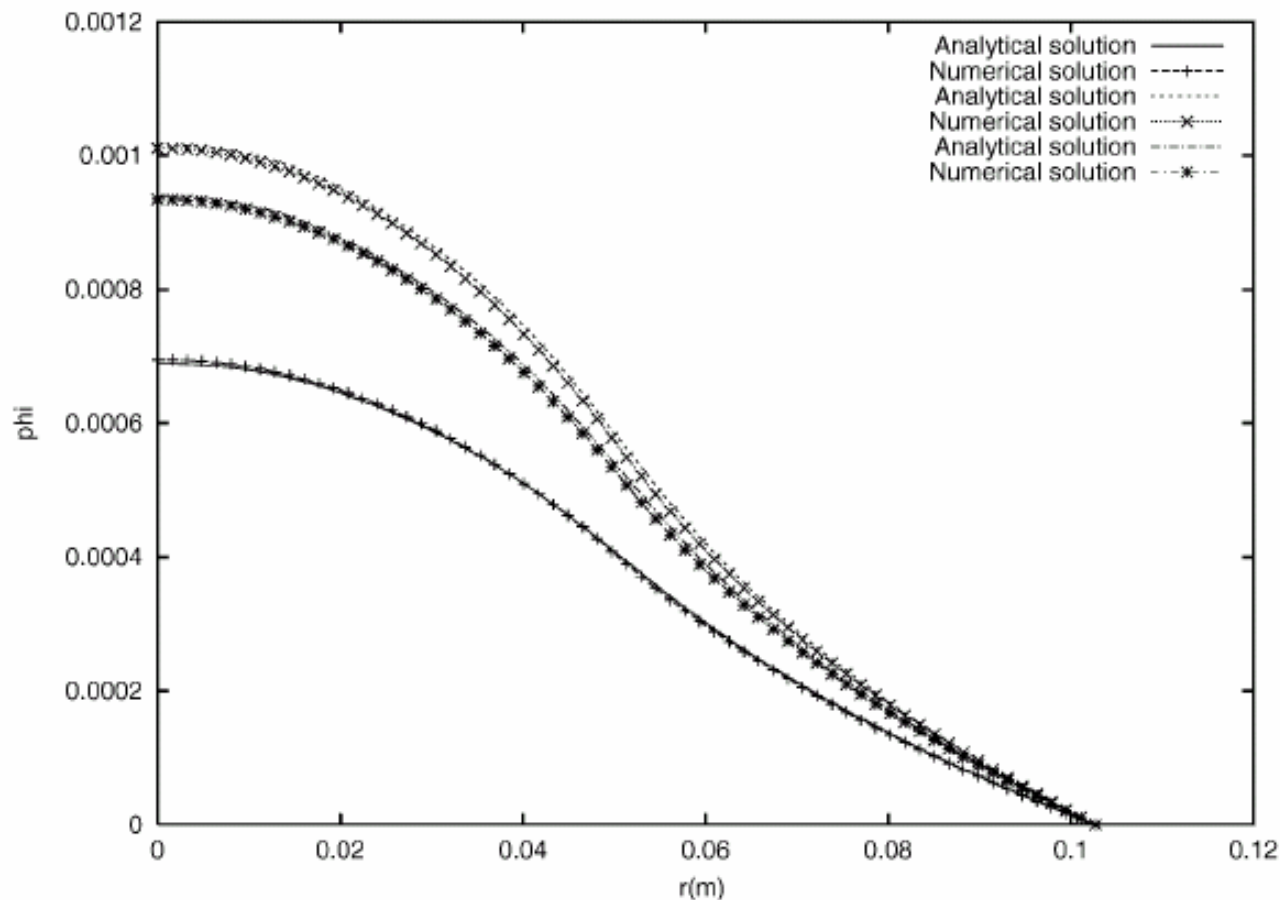
$$\phi^{lm}(z) = \frac{1}{\pi J_m'^2(\gamma_{lm})} \int_0^{2\pi} \int_0^1 \phi(r, \theta, z) \exp(im\theta) r J_m(\gamma_{lm} r) dr d\theta$$

$$\frac{\partial^2 \phi^{lm}(z)}{\partial z^2} - \gamma_{lm}^2 \phi^{lm}(z) = -\rho^{lm}(z) / \epsilon_0$$

$$\frac{\phi_{n+1}^{lm} - 2\phi_n^{lm} + \phi_{n-1}^{lm}}{h_z^2} - \gamma_{lm}^2 \phi_n^{lm} = -\frac{\rho_n^{lm}}{\epsilon_0}; n = 0, 1, 2, 3, \dots, N$$

$$\phi_{-1}^{lm} = \exp(-\gamma_{lm} h_z) \phi_0^{lm}; \quad \phi_{N+1}^{lm} = \exp(-\gamma_{lm} h_z) \phi_N^{lm}$$

# Potential Profiles in a Round Pipe from Analytical Solutions and above Numerical Solutions



(a)

$$E_t(z, t) = \frac{1}{\sin(\beta_0 d)} \left( E_s(z) \cos(\omega t + \beta_0 d - \frac{\pi}{2}) + E_s(z + d) \cos(\omega t + \frac{\pi}{2}) \right)$$

where

$$E_t(z, t) = \sum a_n \cos(\omega t - \beta_n z)$$

$$E_s(z, t) = \cos(\omega t) \sum a_n \cos(\beta_n z)$$

Ref: G. A. Loew, R. H. Miller, R. A. Early and K. L. Bane, SLAC-PUB-2295 (1979).

# External Fields inside the RF Cavity



$$E = - \frac{\partial A}{\partial t}$$

$$B = \nabla \times A$$

$$A_x = \frac{1}{\omega} x \sum_{n=0}^1 \frac{1}{2(n+1)} e_n'(z) r^{2n} \sin(\omega t + \theta_0)$$

$$A_y = \frac{1}{\omega} y \sum_{n=0}^1 \frac{1}{2(n+1)} e_n'(z) r^{2n} \sin(\omega t + \theta_0)$$

$$A_z = - \frac{1}{\omega} \sum_{n=0}^{n=1} e_n'(z) r^{2n} \sin(\omega t + \theta_0)$$

$$e_{n+1} = - \frac{1}{4(n+1)^2} (e_n''(z) + \frac{\omega^2}{c^2} e_n(z))$$

$$F_x(s) = q \int_{-\infty}^{+\infty} W_T(s-s') x(s') \lambda(s') ds'$$

$$F_z(s) = \int_{-\infty}^{+\infty} W_L(s-s') \lambda(s') ds'$$

$$F(s) = \int_{-\infty}^{+\infty} G(s-s') \rho(s') ds'$$

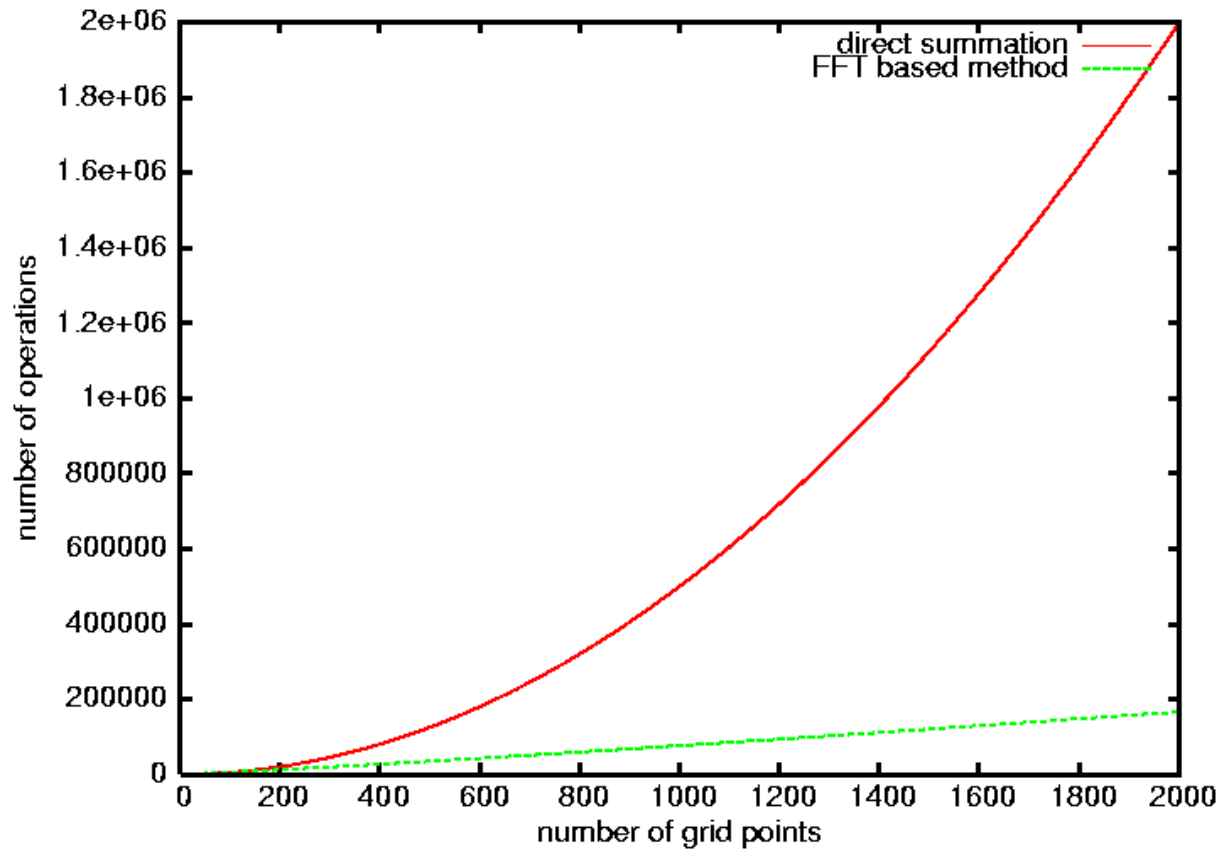
$$G(s) = \begin{cases} W(s) & \text{for } s \geq 0 \\ 0 & \text{for } s < 0 \end{cases}$$

$$F_c(s_i) = h \sum_{i'=1}^{2N} G_c(s_i - s_{i'}) \rho_c(s_{i'})$$

$$F(s_i) = F_c(s_i) \quad \text{for } i = 1, \dots, N$$

# Computing Operation Comparison

between the Direct Summation and the FFT Based Method

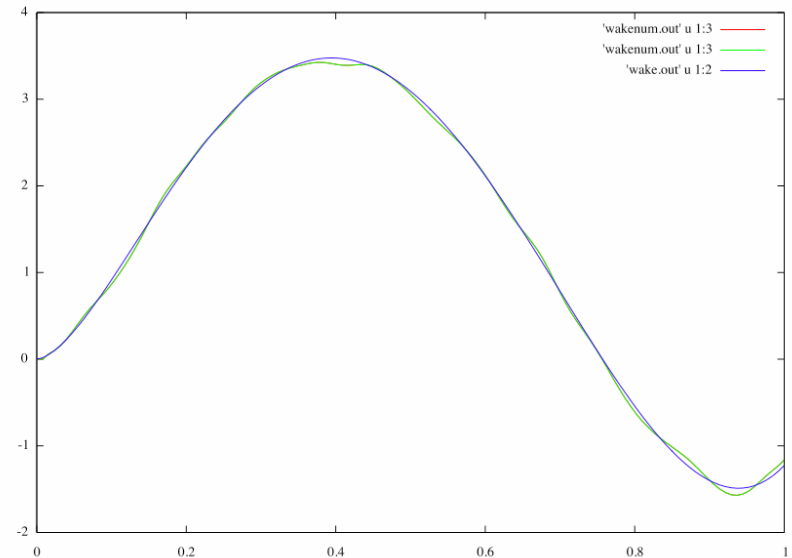
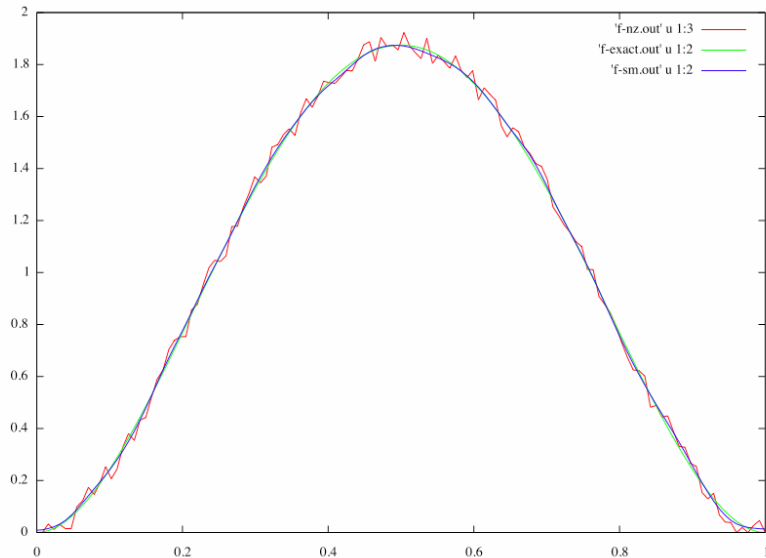


- Steady-state CSR wakefield is used, transient effects not yet included:

$$\frac{dE}{cdt} = -\frac{2e^2}{3^{1/3} R^{2/3}} \int_{-\infty}^s \frac{ds'}{(s-s')^{1/3}} \frac{d\lambda(s')}{ds'}$$

- Numerical evaluation is complicated for two reasons:
  - the integral operator kernel is (weakly) singular; and
  - the 1D charge density  $\lambda(s)$  is contaminated by sampling and discreteness noise (although the

# Multilevel Filtering and CSR Wakes

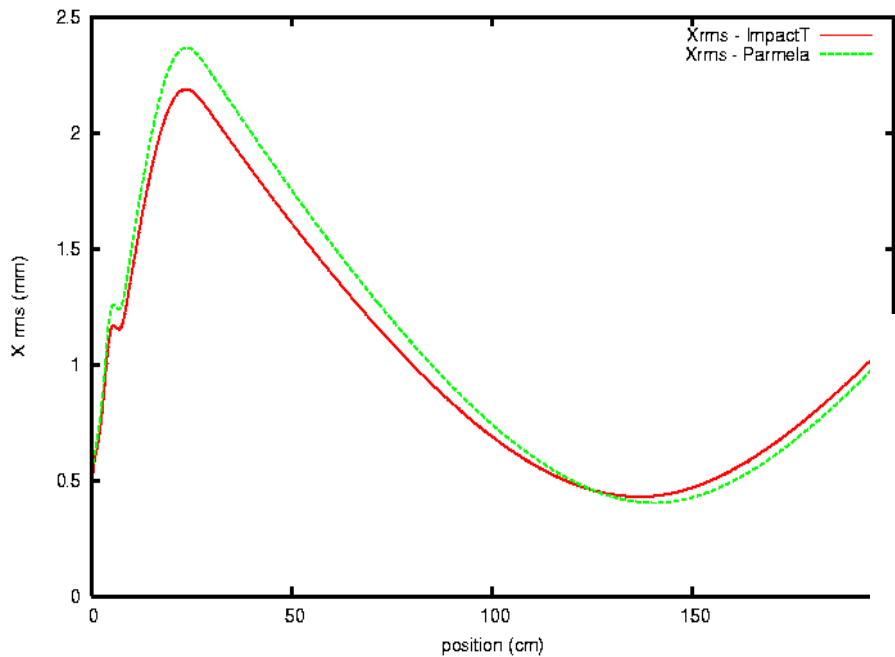


- Choose a low-pass filter that preserves positivity of density, conserves total charge, and is easy to apply, *e.g.*,  
 $(1/96) [7, 24, 34, 24, 7]$
- 2-level denoising: apply first to 2 subsets of length  $N/2$  each, then to 1 set of length  $N$  (the whole of the data)
- $k$ -level: start with  $2^k$  subsamples of length  $N/2^k$ , work down recursively to 1 data set of length  $N$

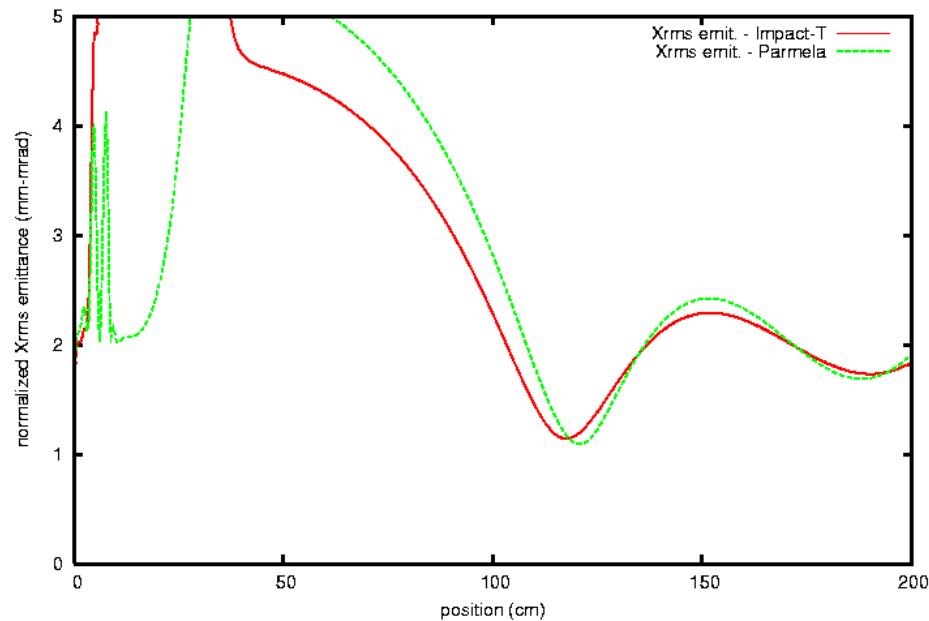
# Benchmark between IMPACT-T and PARMELA



Xrms vs. position with space-charge



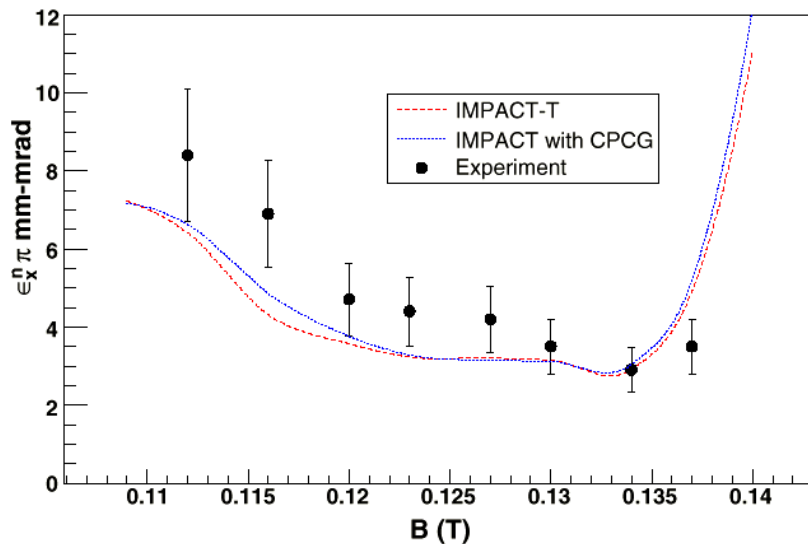
Xrms emittance vs. position with space-charge



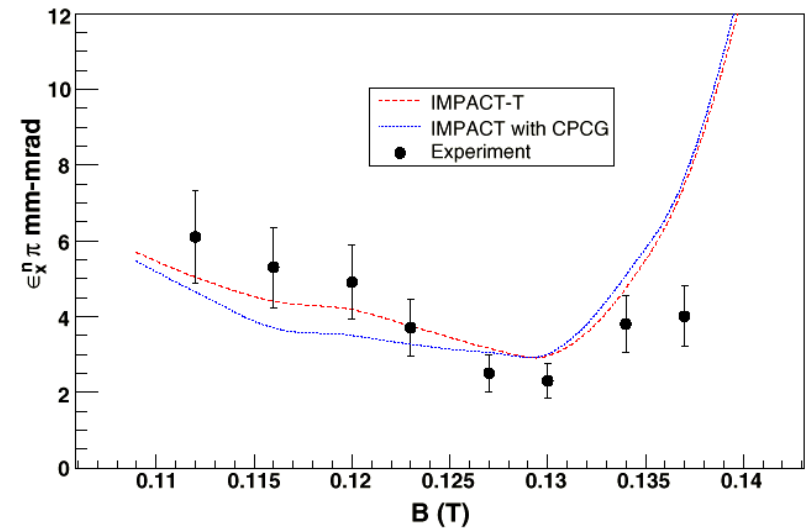
# Comparison of simulation and expt for the FNAL NICADD photoinjector



- NIU/FNAL/LBNL collaboration

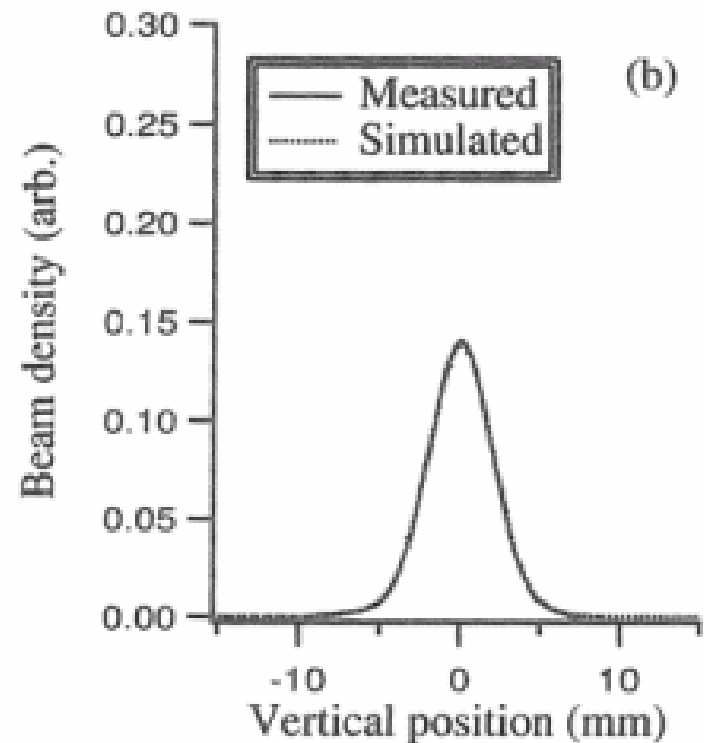
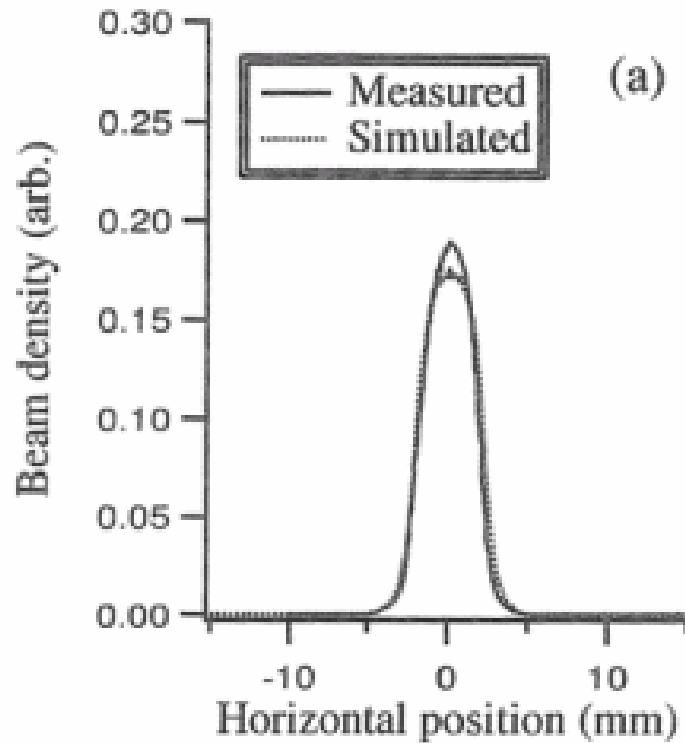
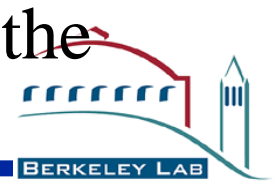


Experimental and simulation results for normalized transverse emittance vs. peak magnetic field inside the gun for single gaussian laser pulses.

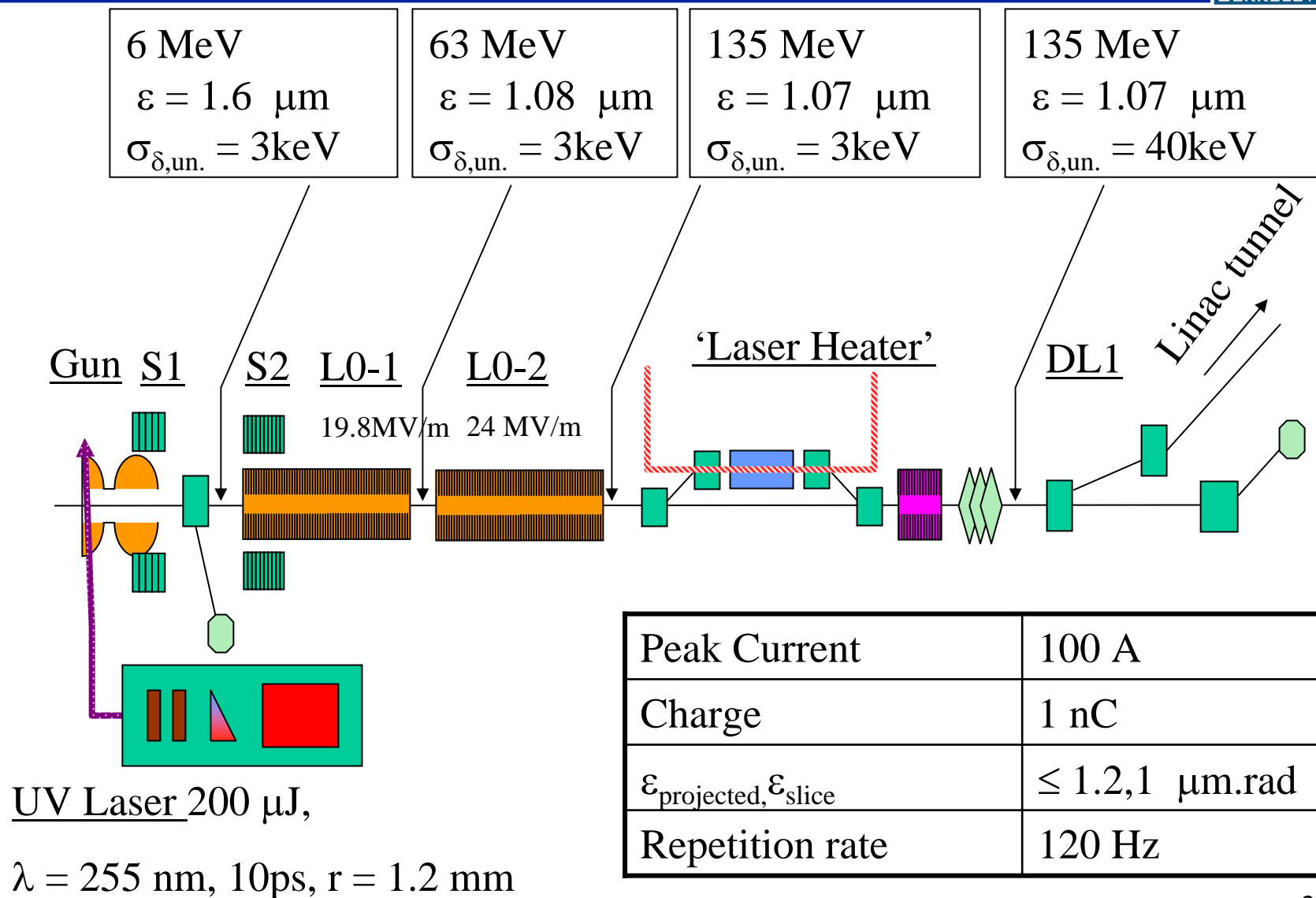


Experimental and simulation results for normalized transverse emittance as a function of peak magnetic field inside the gun for stacked, flat-top laser pulses

# The measured and simulated beam density profiles in the MEBT of J-PARC linac.



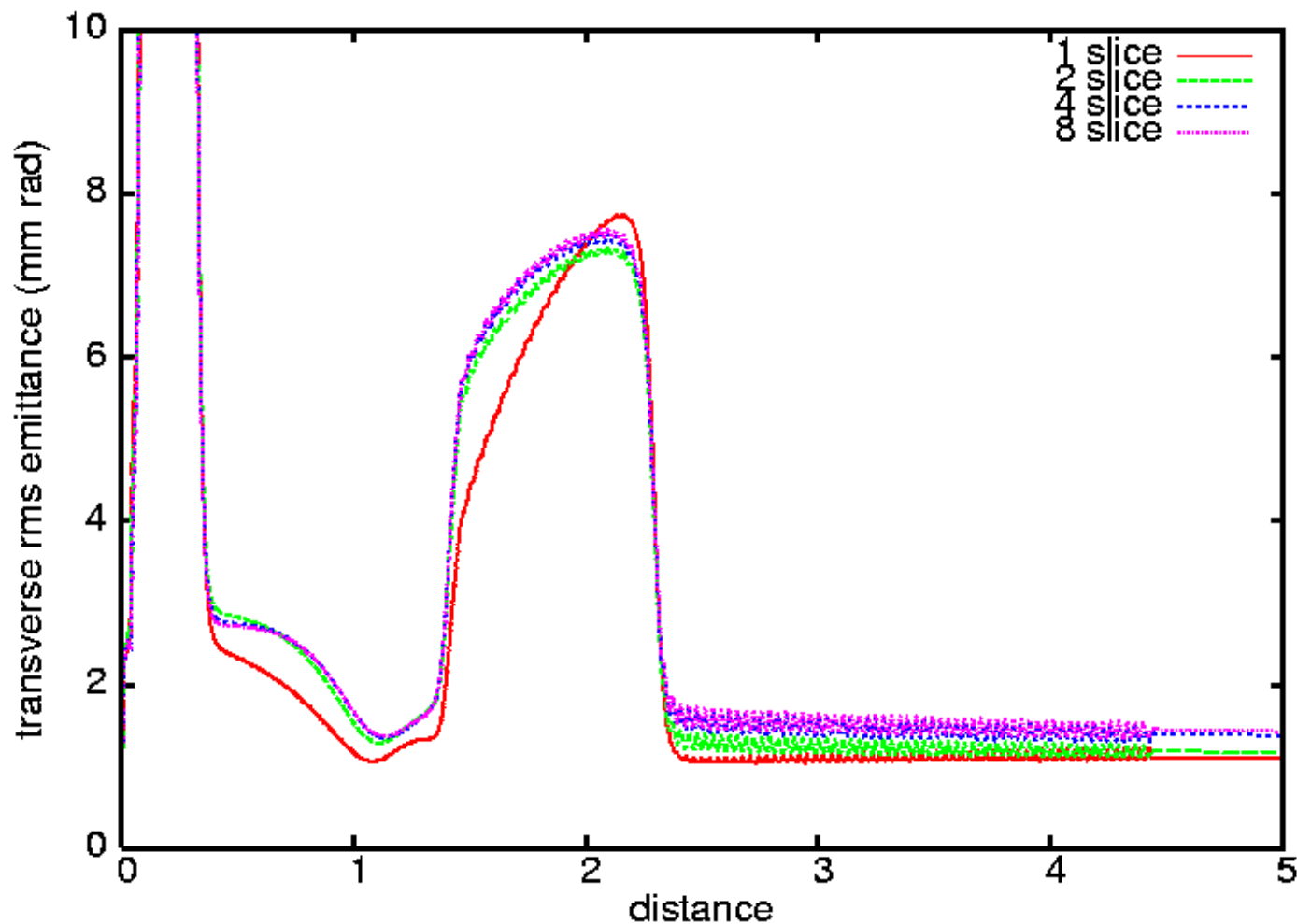
# A Schematic Plot of LCLS Injector Layout



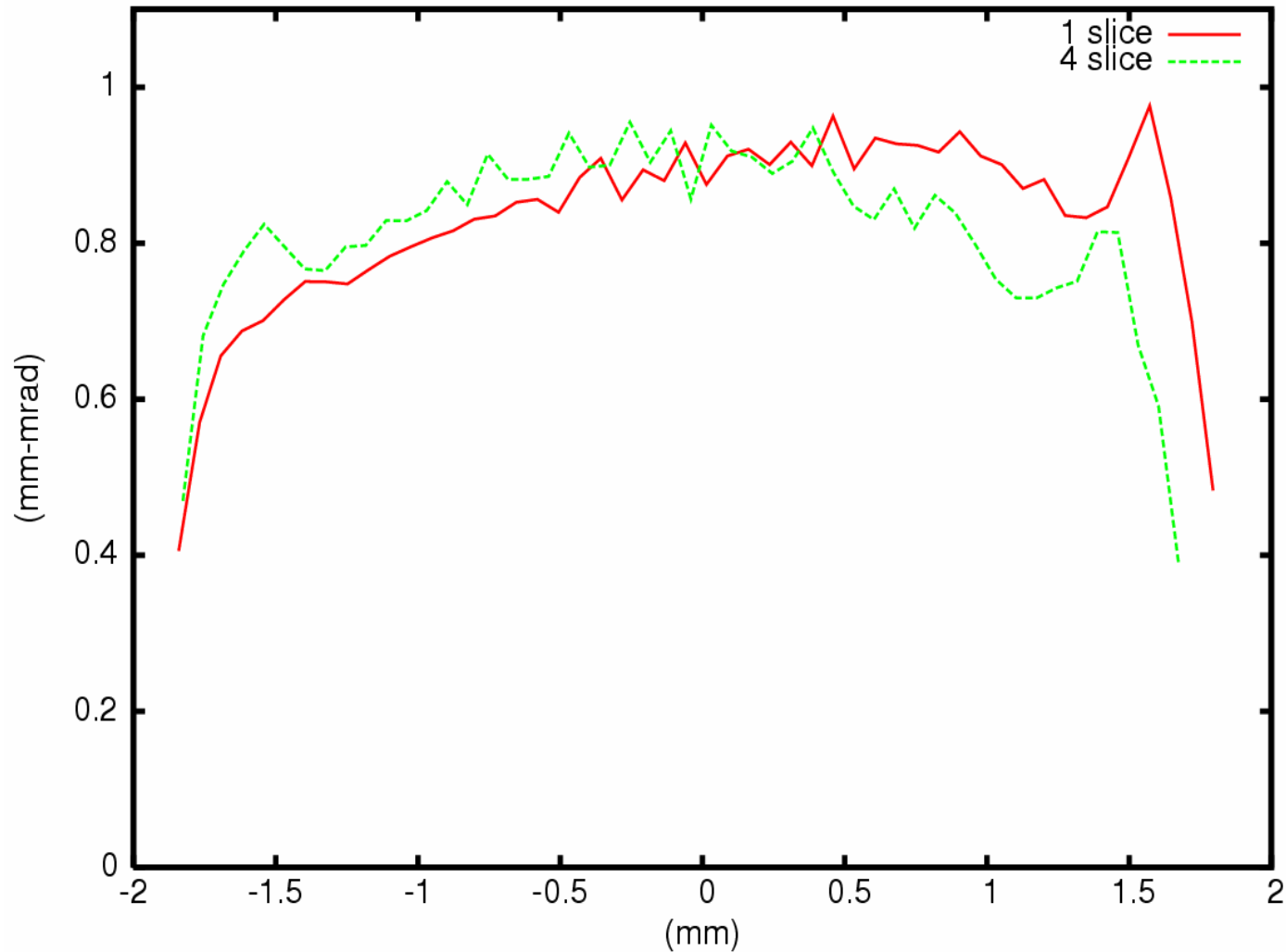
# Transverse Emittance vs. Distance Using Multiple Slices



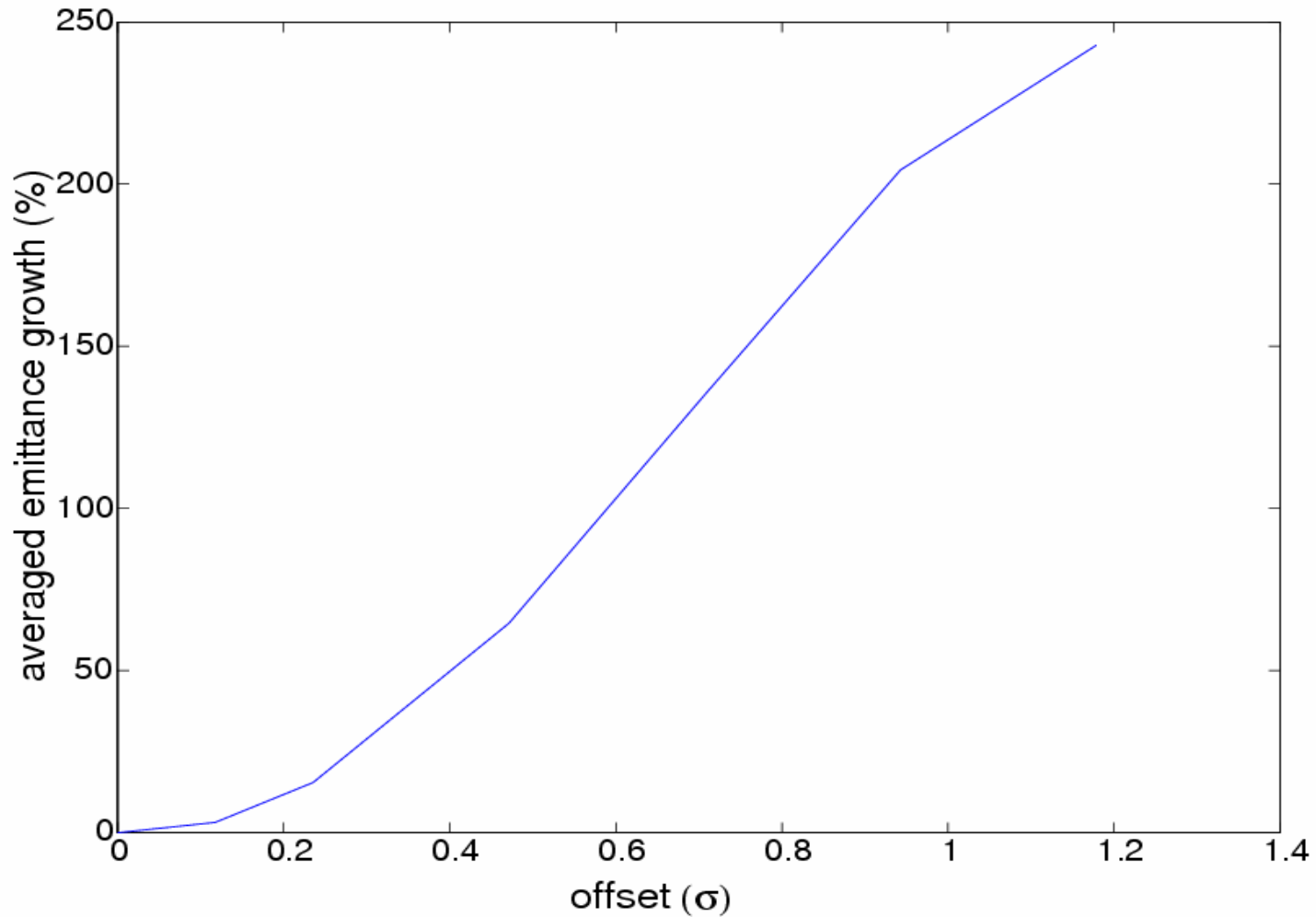
30% more final emittance growth than single slice model

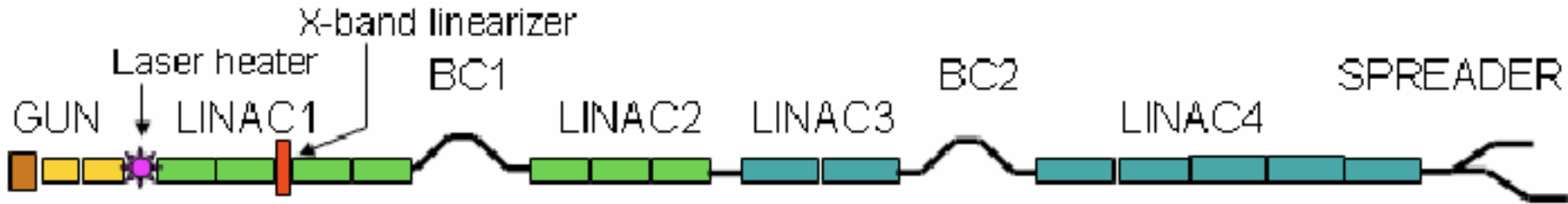


# Transverse Sliced Emittance after the L0-1 with Different Longitudinal Slices



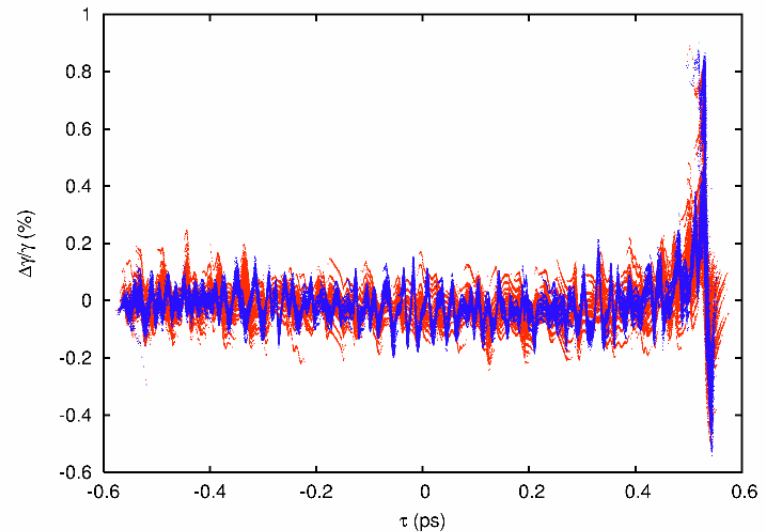
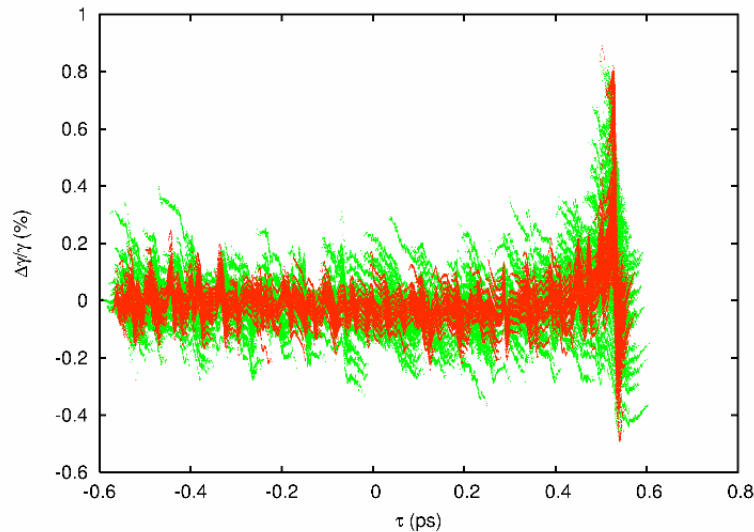
# Emittance Growth after L0-1 vs. Initial Offset





- Beam energy at the entrance of laser heater  $\sim 100$  MeV (peak current  $\sim 70$  A), at the exit of Linac 4  $E \sim 1.2$  GeV (peak current 500 A or 800 A depending on configuration)
- Medium bunch (0.7 ps) and long bunch (1.4 ps) options
- 2 bunch compressors, 4 linacs (a total of 15 RF cavities), followed by a spreader used to direct the beam into one of two undulator lines

# Microbunching Instability vs. Macroparticle Number

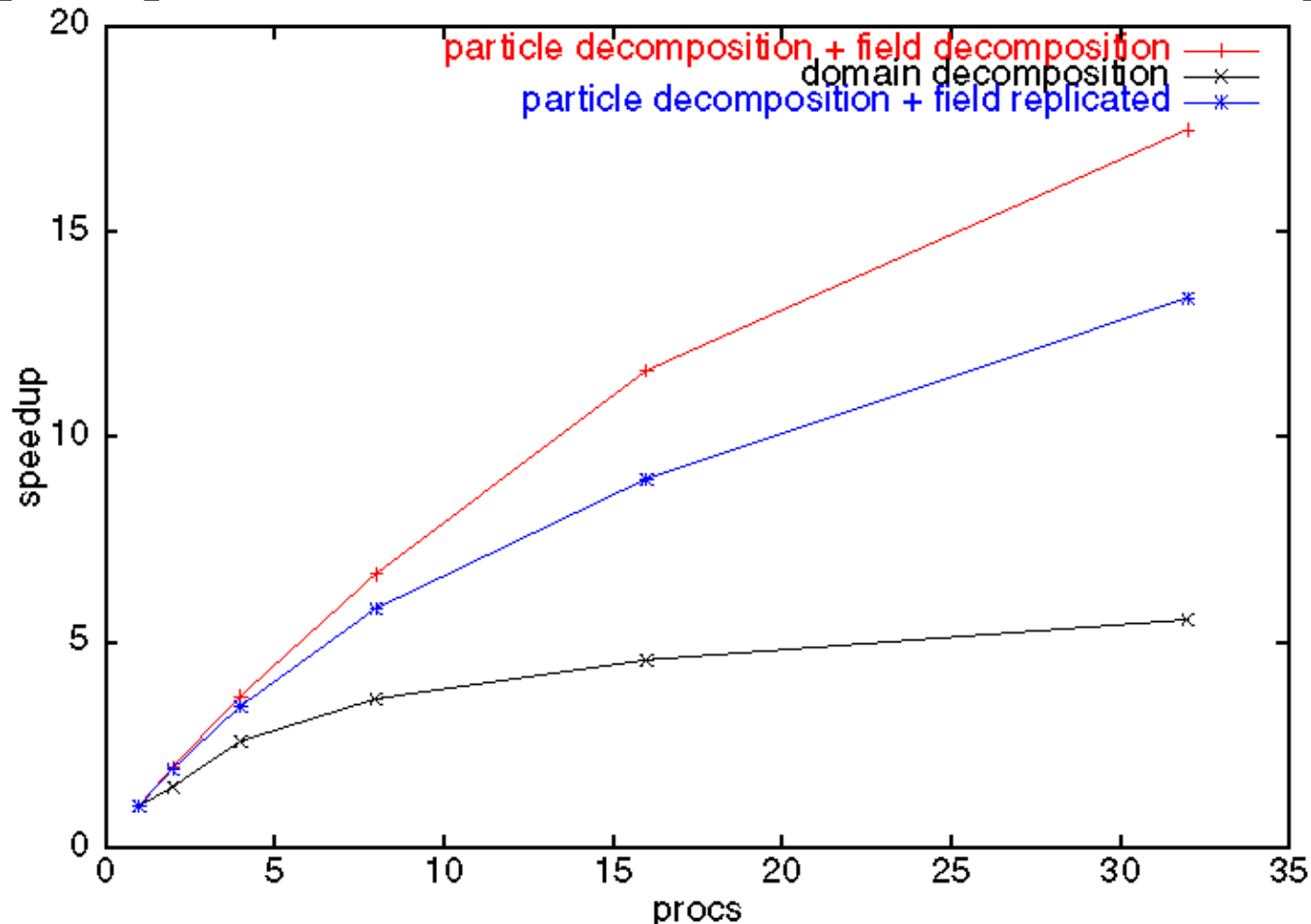


- Same initial distribution is sampled by 2M (left, green), 20M (left and right, red), and 100M particles (right, blue)
- Same initial slice energy spread of 7.7 keV grows to 940keV/530keV/360keV in simulations with 2M/20M/100M particles
- Data from simulations in the 2M-100M range is insufficient to determine the limiting behavior, if any; larger runs are needed

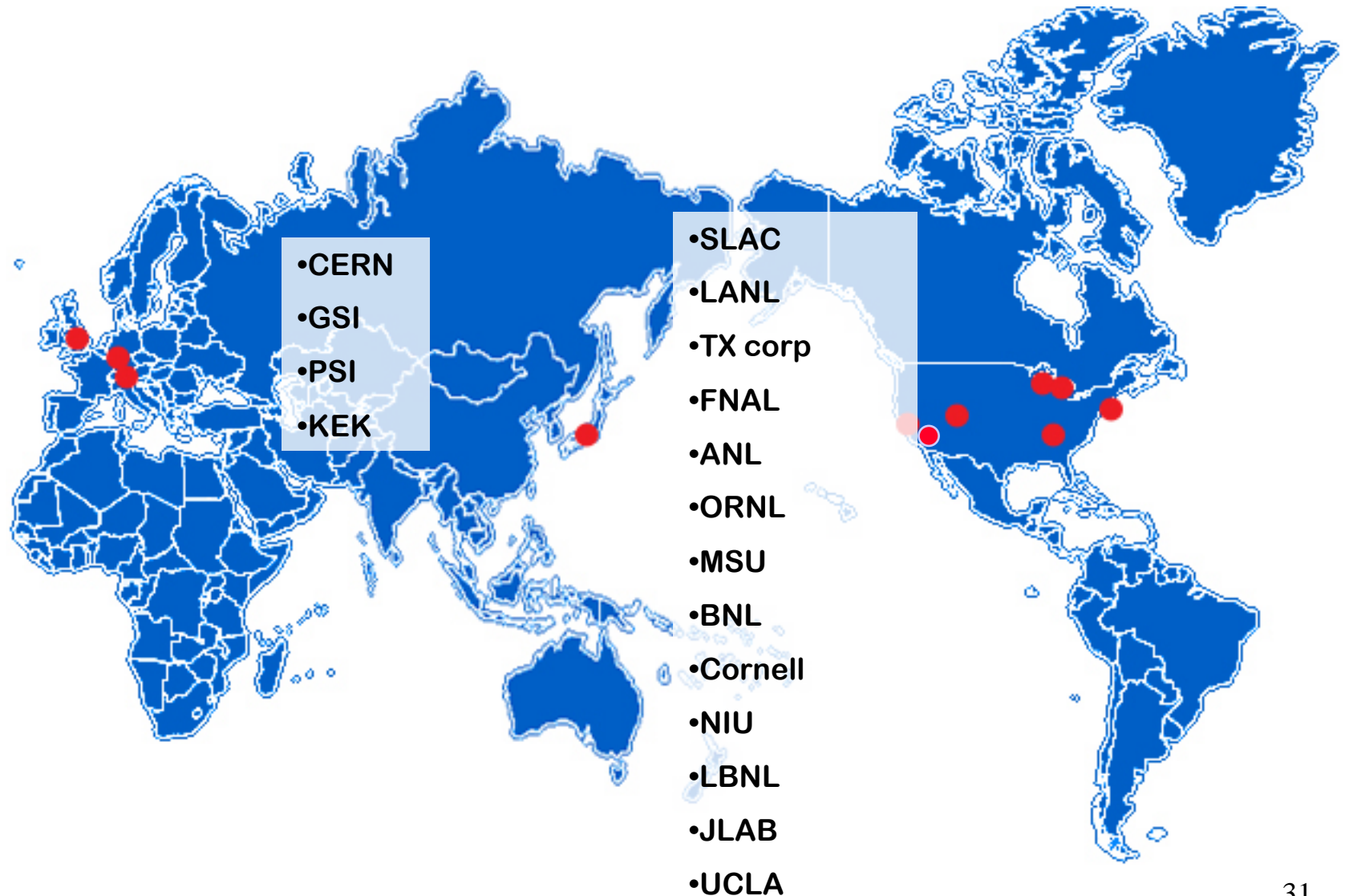
# Parallel Implementation: Performance vs. Implementation Methods



## Speedup vs. Number of Processors with Three Decomposition



# IMPACT User-Map



# Acknowledgements



LANL – S. Habib

LBNL – M. Furman, S. Lidia, I. Pogorelov, R. Ryne, A. Zholents

SLAC – C. Limborg

KEK – M. Ikegami

UCLA – V. Decyk

FNAL/NIU – D. Mihalcea

And feedback from many IMPACT suite users

Work performed under the auspices of the  
**DOE SciDAC Accelerator Project** using resources at the  
**National Energy Research Scientific Computing Center**